Science of the Total Environment 782 (2021) 146886

Contents lists available at ScienceDirect

Science of the Total Environment

journal homepage: www.elsevier.com/locate/scitotenv

Remote estimation of aquatic light environments using machine learning: A new management tool for submerged aquatic vegetation

Ryan M. Pearson [a,*], Catherine J. Collier [b], Christopher J. Brown [a], Michael A. Rasheed [b,c], Jessica Bourner [d], Mischa P. Turschwell [a], Michael Sievers [a], Rod M. Connolly [a]

[a] Coastal and Marine Research Centre, Australian Rivers Institute, School of Environment & Science, Griffith University, Gold Coast, Queensland 4222, Australia
[b] Centre for Tropical Water and Aquatic Ecosystem Research, James Cook University, Cairns, Queensland 4870, Australia
[c] College of Science and Engineering, James Cook University, Cairns, QLD 4870, Australia
[d] Gold Coast Waterways Authority, Australia

HIGHLIGHTS

- Human activities affect the light that submerged vegetation needs to survive.
- Machine learning (ML) can estimate light and inform ecological management.
- Our ML-derived submerged vegetation light model (SVLM) is >99% accurate.
- The SVLM can be used to adaptively manage submerged habitats.

GRAPHICAL ABSTRACT

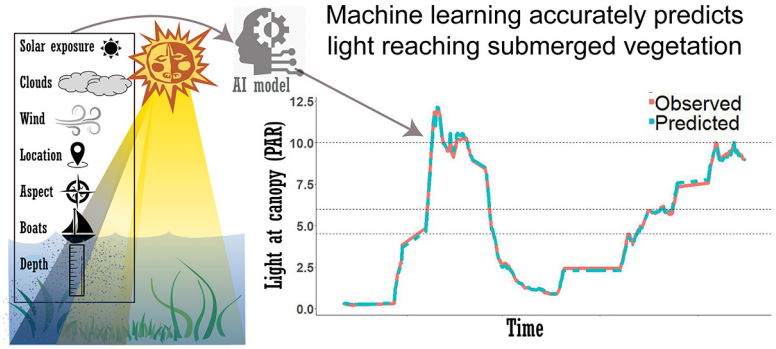

ARTICLE INFO

Article history:
Received 18 January 2021
Received in revised form 10 March 2021
Accepted 28 March 2021
Available online 1 April 2021

Editor: Christian Herrera

Keywords:
Seagrass
Light requirements
Irradiance
Impact management
Thresholds
Dredging
Zostera
SAV

ABSTRACT

Submerged aquatic vegetation (SAV; e.g. seagrasses, macroalgae), forms key habitats in shallow coastal systems that provide a plethora of ecosystem services, including coastal protection, climate mitigation and supporting fisheries production. Light limitation is a critical factor influencing the growth and survival of SAV, thus it is important to understand how much light SAV needs, and receives, to effectively assess the risk that light limitation poses. Light monitoring is commonly used to inform environmental decision making to minimise loss of SAV habitat, but the temporal and spatial extent of monitoring is often limited by cost and logistical difficulties. An ability to remotely estimate light across different locations can therefore improve the conservation and management of SAV habitats. Here we combine an extensive monitoring program with publicly available data and machine learning to develop a model that estimates the light reaching submerged seagrasses in a shallow subtropical embayment in southern Queensland, Australia. Our model accurately predicts the intensity of photosynthetically active radiation (PAR) reaching the canopy of SAV from entirely remotely available data. The best performing model predicted light intensity with >99% at the management relevant daily, and 14-day rolling average time resolutions. This model enables monitoring of light available to SAV without an ongoing need for in-water instruments, minimising cost and risk to personnel, and improving assessment speed. The technique can be applied to SAV management plans in shallow waters throughout the world, where suitable remote public data is available.

* Corresponding author at: Australian Rivers Institute, School of Environment and Science, Griffith University Gold Coast Campus, Parklands Drive, Gold Coast 4222, Queensland, Australia.
E-mail address: r.pearson@griffith.edu.au (R.M. Pearson).

https://doi.org/10.1016/j.scitotenv.2021.146886
0048-9697/

1. Introduction

Coastal habitats characterised by the presence of submerged aquatic vegetation (SAV), such as seagrass and macroalgae, play important roles in supporting biodiversity, and providing ecosystem services including carbon storage, fisheries, and coastal protection (Scott et al., 2018; Brown et al., 2019; Sievers et al., 2019). But coastal SAV ecosystems are under threat, and while some areas are showing signs of recovery (de los Santos et al., 2019), SAV ecosystems are declining in extent at a global scale, largely as a result of human-driven disturbances (Orth et al., 2006; Waycott et al., 2009). Globally, human activities and natural phenomena can affect habitat suitability for SAV, especially through changes to the light environment by increasing turbidity (Anthony et al., 2004; Lawson et al., 2007). Land-use changes can increase erosion, nutrients, and contaminants in waterways and changing climactic conditions can increase wind, rain and storm events. As well as other effects, each of these can affect SAV health by increasing turbidity which reduces light penetration through the water column, potentially causing light-stress (Lawson et al., 2007).

To help reverse losses and inform management of these habitats, there is need to monitor and manage important environmental parameters linked with SAV persistence. The dynamic and complex nature of environmental conditions in SAV ecosystems make monitoring difficult and sometimes dangerous, leading to high time and monetary cost involved in research and management, and limited time-series data available for long-term comparisons (Kilminster et al., 2015; Sievers et al., 2020). Thus, effective management of these ecosystems would benefit from a low-cost method to rapidly assess critical factors that cause changes in habitat suitability.

Light, or more specifically, photosynthetically active radiation (PAR) reaching the canopy of SAV, affects their growth and survival (Lee et al., 2007; Collier et al., 2016b). Light stress can occur naturally, but the frequency and intensity of light stress events can also increase due to human activities (Garrad and Hey, 1987; Ganju et al., 2014). In complex coastal waters, weather events (e.g. wind, rain, large storms) can reduce light levels for relatively long periods (Lawson et al., 2007), potentially affecting the resilience of submerged vegetation to additional stress (Yaakub et al., 2014). Assessing the light reaching SAV has traditionally relied on costly in-water measurements that provide observations limited to specific places in space and time (Collier et al., 2012a; Chartrand et al., 2016). Further, some historical assessments have relied on inaccurate proxies (e.g. secchi disks), leaving a paucity of existing comparable time-series data for long-term assessments linking pressures to ecosystem health. Modern in-water techniques (e.g. light loggers) to quantify light intensity have improved accuracy and ability to understand change over time, but necessary repeat visits to locations for instrument maintenance also requires considerable effort. This limits the ability for managers to employ adaptive strategies that allow rapid response to changing conditions and adequate spatial coverage to determine potential impacts. Remote sensing technologies have improved capacity for rapid assessments across large spatial scales by allowing collection of time-series data for many variables (Álvarez-Romero et al., 2013; Roelfsema et al., 2014; Magno-Canto et al., 2019; Coffer et al., 2020; Zoffoli et al., 2020). However, applying remote techniques for SAV management can be hampered due to the numerous drivers that impact coastal water clarity, the shallow depths where SAV typically occurs, and limitations in the techniques to adequately account for these.

Coastal water quality and light reaching SAVs can be affected by a plethora of natural and human processes (e.g. Lawson et al., 2007). For example, periods of high rainfall, strong winds and wave energy often increase suspended materials, reduce light penetration and potentially cause short-term light-stress to SAV. Conversely, calm waters during sunny periods may offer respite to SAV, allowing photosynthetic processes to rebuild energy stores, increase growth rates and enable survival (Anthony et al., 2004; O'Brien et al., 2018). The complex interactions between these processes result in highly variable light intensities to which SAV have adapted, to some extent, by displaying morphological and physiological plasticity (Maxwell et al., 2014). However, prolonged periods of time below light requirements can affect the growth and survival of SAV (Wu et al., 2018). The frequency, intensity, or duration of excursions below light requirements can be exacerbated by human activities (Collier et al., 2012b; McMahon et al., 2013; York et al., 2015; O'Brien et al., 2018), with chronic low-light reducing resilience to further light-stress (Yaakub et al., 2014). Thus, any additional stress beyond natural cycles (e.g. from boat generated wake, sand management) can surpass tolerance thresholds and trigger reductions in growth and survival. Having a capacity to remotely, and accurately, estimate light intensity would mean that the effect of various processes affecting light can be measured, risk to habitat identified, and processes or activities influencing light managed.

Consideration of the natural and human influences on water quality are key components of water quality and SAV management (Dixon, 1999; Erftemeijer and Shuail, 2012; Chartrand et al., 2018). Models that account for these can be used to predict habitat suitability (Baird et al., 2016), to identify water quality constituents (Fernandes et al., 2018; Fernandes et al., 2019), or activities (Chartrand et al., 2016) to be targeted for management. Water quality models can provide a wide spatial coverage, and can be used to hind-cast, enabling comparisons of current and historical habitat suitability.

Here, we aim to use remotely available environmental data to develop a machine learning model that accurately predicts light reaching SAV at management-relevant spatiotemporal resolutions in a subtropical estuary. We further aim to test the sensitivity of predictions to variations in training data quantity and spatiotemporal coverage. Having access to an accurate modelling solution will allow researchers and managers to minimise cost, effort, and risk (to both humans and equipment) associated with monitoring and managing SAV. Modelled approaches also provide the ability to hindcast conditions to support assessments of past environmental change (e.g. Kerimoglu et al., 2018).

2. Methods

We undertook an extensive monitoring program to measure 'natural' light intensities and understand the influence of natural and human influences on light in our case-study location – the Gold Coast Broadwater in southern Queensland, Australia (Fig. 1). The Gold Coast Broadwater is the southern-most section of Moreton Bay, a shallow sub-tropical embayment in eastern Australia. It is surrounded by urban area that is home to more than 600,000 people (City of Gold Coast, 2019), agricultural lands, and extensive made-made canal systems. The waterway experiences high boating traffic, especially during holiday periods (Leon and Warnken, 2008). Largely protected from oceanic swells, the Broadwater is home to eight seagrass species, which cover approximately 1200 ha (Cuttriss et al., 2013; Connolly et al., 2016). *Zostera muelleri* is the most prevalent species (Sievers et al., 2020), growing from the intertidal zone to approximately 3 m depth (Connolly et al., 2016). Locally relevant light thresholds were recently established for subtidal *Zostera muelleri* in the Gold Coast Broadwater (Pearson et al., 2020). In this region, managers are advised to implement sand management mitigation measures if activities caused light intensity to fall below a two-week rolling average of 4.5 mol/m^2/d (Connolly et al., 2016; Pearson et al., 2020). Thus, we include this threshold and time-period as one of 11 levels in model accuracy assessments (described in data processing & analysis section).

2.1. Light measurements in seagrass meadows

We measured light intensity (in 1-minute intervals) and water depth (4–16 measurements/s, averaged to 1-minute intervals for analyses) within seagrass meadows over 13 months (Sep 2018 to Oct 2019). We were interested in biologically active wavelengths, and thus installed Odyssey photosynthetically active radiation (PAR) light

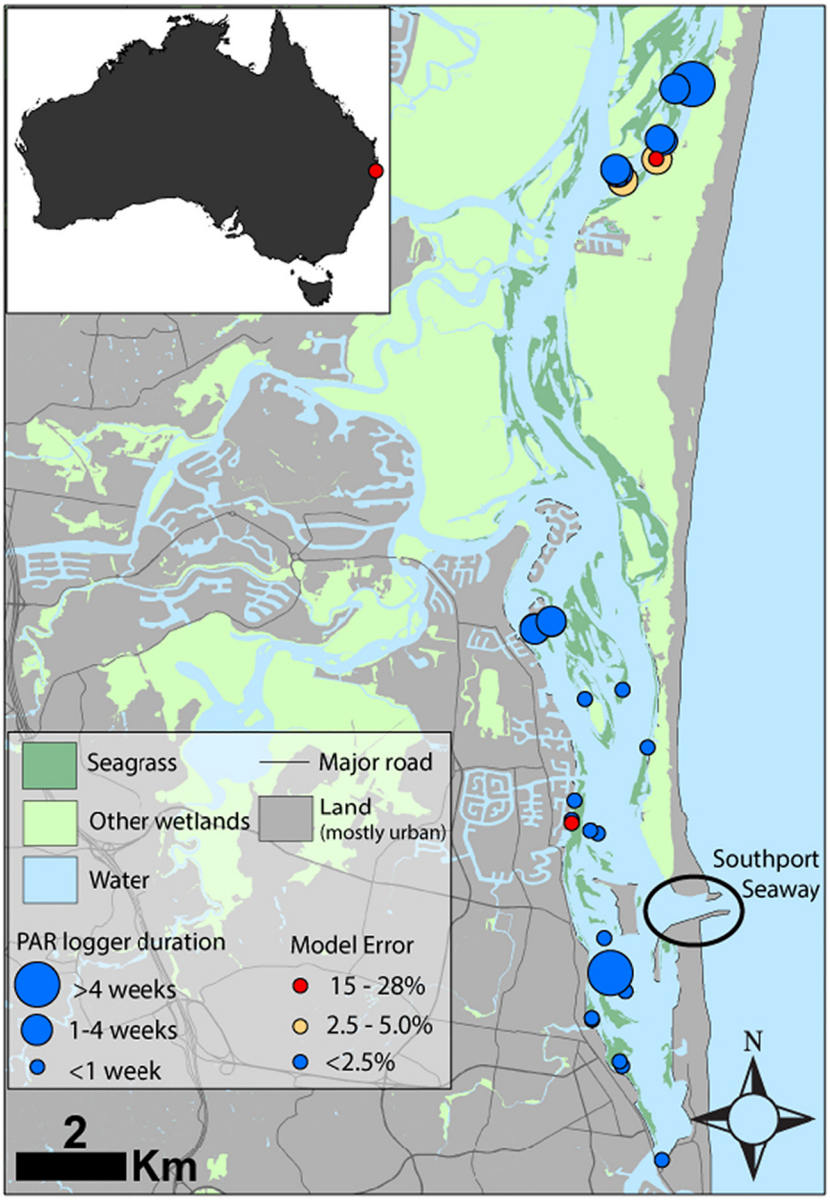

Fig. 1. PAR logger deployment locations in the Gold Coast Broadwater. Circle size and colour are categorical representations of duration of in-water measurements (size) and mean site-error (colour; as mean difference between observed and predicted values by the best model (designated K1). Seagrass layer from Cuttriss et al. (2013). (For interpretation of the references to colour in this figure legend, the reader is referred to the web version of this article.)

loggers in concert with Ruskin RBR depth loggers in 31 locations for periods ranging from hours to several weeks (Figs. 1; S2.2). Automatic wiper units (Zebra-tech models) were installed to maintain clean sensors throughout the monitoring period. The maximum depth observed at any site was 3.43 m, and the average maximum depth across all deployments was 1.46 m ± 0.17 m (mean ± SE). At any point in time, up to 6 units were deployed simultaneously between Sep 2018 and Oct 2019. Data were collected across the full suite of environmental conditions experienced in the Broadwater: during the dry season and periods of peak summer rainfall (including during exposure to an ex-tropical cyclone in February 2019); across quiet weekdays, weekends and busy holiday periods (e.g. Christmas, Australia Day and Easter) when boating traffic is expected to be much higher than during regular weekdays; throughout all tidal cycles (spring and neap tides); under calm and strong winds, and; with a variety of day-lengths through Spring, Summer, Winter and Autumn. Thus, light data collected is representative of a variety of environmental and boat traffic conditions in the survey area.

2.2. Data processing & analyses

We used the in-water observation data in concert with publicly available data to develop a Submerged Vegetation Light Model (SVLM) to estimate light intensity at the SAV canopy. Light was the response variable and 11 remotely available or calculable variables were predictors (Table 1). We assigned each 1-minute light measurement a value for each of 11 predictor variables (Table 1) that are known locally and/or globally to influence light strength or penetration through the water column (Maxwell et al., 2017; O'Brien et al., 2018; Wu et al., 2018). Predictor variables, their data source, and the temporal resolution used are listed in Table 1, with detailed descriptions of each provided in S1. Solar dose was re-calculated to 1-minute resolution from a daily solar exposure value (described in detail in S1). For all other predictors, when the temporal resolutions did not align, we applied values for the coarser time-scale in each data source to each 1-minute observation. This means that all 1-minute observations within a single day received the same value for a 'daily' predictor, such as the Lti or rainfall.

Table 1
Predictor variables used in modelling of light levels in the Submerged Vegetation Light Model (SVLM). BoM: the Australian Bureau of Meteorology. Detailed descriptions and reasoning for each predictor are in Supplementary S1.

Predictor	Data source	Observed range	Units	Temporal resolution
Boating intensity	Proxy used (Leisure time index[a]; adjusted)	1–23	Categorical	Daily
Cloud cover	BoM (Coolangatta station[b])	0–8	Okta	1 min
Depth	Several - In-situ measurements and calculations based on offsets from Tide height	0–3.43	m	1 min
Distance from ocean inlet	Straight-line distance in metres, measured using Google Earth	1888–15,110	m	Static
Rainfall (3-day cumulative)	BoM (Seaway station)	0–300	mm	Daily
Site aspect	Direction from centre of channel towards near-shore logger location, perpendicular to shoreline	0–325	Degrees	Static
Solar dose	Calculated from BoM daily Solar exposure using sine wave conversion	0.000–0.0059	$MJ/m^2/min$	1 min
Tide direction	Calculated from tidal data	Decreasing, slack low, increasing, slack high	Categorical	1 min
Week	Calculated Julian week in sequence through year (values 1 to 53, starting 1 January)	1–53	Integer	1 week
Wind direction	BoM (Seaway station)	0–359	Degrees	1 min
Wind speed	BoM (Seaway station)	0–85	km/h	1 min

[a] Adapted from Leon and Warnken (2008).
[b] Coolangatta weather station, at ~16 km (linear) from the Gold Coast Broadwater is the closest station that measures cloud cover.

The temporal resolution listed in Table 1 is representative of the value applied to each 1-minute observation in the model. Additional variables (e.g. suspended solids and sediment grain size) are also likely to affect light availability (Adams et al., 2016) but were not included in this analysis due to an absence of remotely available or calculable data at appropriate resolutions.

We used a generalized boosted regression modelling (GBM) technique, with the gbm package in R (Greenwell et al., 2019) to analyse these data and develop predictive models. These analyses use an iterative machine learning process to train a model to predict a response variable (in this case PAR) based on conditions related to the influence of a set of predictor variables (Elith and Leathwick, 2017). A training dataset is used to determine the influence of various predictor variables on the response variable by randomly permuting each predictor variable and computing the associated reduction in predictive performance. We tested prediction accuracy in two ways:

1. against a randomised subset of the training dataset with 80% of the training dataset assigned to training the model and 20% to estimate squared error loss in each iteration (Elith and Leathwick, 2017). This enables the model to improve through an iterative process and identify the iteration with the best predictive accuracy, and;
2. against an independent dataset that was not provided to the model.

If training data are sufficiently representative of a broad range of conditions, the model is able to learn how each predictor influences the response and apply these influences to estimate values for new datasets, making this the ideal technique for the purpose. We note that GBM models are robust to multicollinearity due to the iterative process in which GBM builds regression trees, ensuring that redundant variables are never selected (Elith and Leathwick, 2017). There is thus no benefit in subjectively deciding a-priori whether variables should be excluded based on correlations between variables. GBMs handle interactions between predictors well and are capable of handling missing data in predictor variables. Therefore, while some of our predictors interact with one another (e.g. wind direction and site aspect), the influence that each exerts on measured light intensities justifies inclusion of all.

Data pre-processing involved exclusion of night-time periods (to precise sunrise-sunset times for each day from local data provided by BoM) to allow the relative influence of predictors to be assessed appropriately, undiluted by night-time comparisons for which they have no effect. This resulted in a daytime light intensity dataset containing 386,928 light observations at 1-minute intervals from 268 dates. Prior to training the model, the full dataset was split into separate training and testing datasets using random assignment of whole days. Following model training, the testing dataset was used as the independent data to test the accuracy of the model.

The SVLM was processed at the 1-minute resolution, ensuring maximum training data were used and that the effects of short-term influences were captured within the model. Due to limitations with some data sources, this may have introduced some temporal mismatches between the predictor and in-situ observations, especially for factors where temporal and spatial differences exist between logger location and the place of predictor measurement. For example, cloud cover was measured at the nearest available weather station (25–40 km away from nearest and farthest logger locations). Similarly, some other variables (e.g. boating, cumulative 3-day rainfall) were only available as daily estimates or proxies. We expected short-term temporal mismatches in predictor variables to balance over longer periods, minimising overall error at daily resolution and longer. Thus, we assessed model accuracy at multiple temporal resolutions relevant to management decisions. We summed all observations within a day to calculate daily doses for both observations and predictions (separately), converting units from $\mu mol/m^2/s$ to $mol/m^2/d$) using:

$$mol/m^2/d = (\text{sum}\ (\text{daily}\ \mu mol/m^2/s{*}60))/1,000,000$$

Optimum model input parameters were determined using the gbm.tune function. This function tests the accuracy of the model against different combinations of input parameters that can be defined by the user. These include variations in the number of trees, minimum observations per node, training proportion, bag fraction, tree complexity, cross-validation folds and more (Table S1). We tested 24 different combinations of the parameters and used the set of parameters that returned the lowest root-mean-square error (RMSE) as our primary model (Table S1).

A gbm object was created using the training dataset and then used to predict light intensity from predictor variables in the independent testing dataset. We assessed model accuracy using linear regression of observed vs predicted light intensity at both the 1 min and daily resolutions, assessing R^2 and RMSE for model accuracy. We also plotted daily values in time-series to visualise accuracy over time. We additionally calculated a 14-day rolling average, the resolution commonly used by managers to trigger management actions. Several light thresholds for the management of seagrasses during sand management activities have been recommended in Queensland (e.g. 10 & 6 $mol/m^2/d$ (Chartrand et al., 2016)), and recent work in Gold Coast *Zostera muelleri* meadows recommended a 4.5 $mol/m^2/d$ threshold (Pearson et al.,

2020). We use these thresholds as visual guides when plotting daily dose predictions to demonstrate accuracy against specific regionally relevant thresholds. We then compared predictions and observations against 11 pre-defined real and hypothetical management thresholds: integer values between 1 and 10 mol/m^2/d; as well as the locally defined 4.5 mol/m^2/d threshold. We calculated the number of times the model predicted light on the correct side of each threshold (i.e. matching whether the observed value was above or below) as well as the number of false low (incorrect prediction under threshold) and false high (incorrect prediction above threshold) predictions.

2.3. Sensitivity analyses

We tested sensitivity to training data quantity and spatiotemporal coverage by separating the full dataset into training and an independent testing datasets by several means. To test the effect of data quantity on model accuracy, we split the full dataset using nine proportional levels, whereby X% of days were assigned to training and the remaining Y% were used to test the accuracy of predictions at the daily and sub-daily level. In other machine learning analyses it is common that 80% of data is assigned to training a model (Alexandropoulos et al., 2019), thus high accuracy at any level below 80% training data would imply the model is robust. The nine levels had 75%, 50%, 40%, 30%, 25%, 10%, 7.5%, 5%, and 3% of days assigned to training the model and were repeated between 3 and 6 times for each level and number of predictors. These data were assigned randomly, with the intention of testing accuracy within the temporal range of the training data. The best model was designated as the most accurate at predicting against management thresholds and was repeated 5 times, using different randomised separation of training & testing datasets to test the replicability of the model. The full dataset (combined training and testing) was required to test accuracy against management relevant thresholds, given the need to calculate 14-day rolling averages for this analysis. Typical outputs from these five replicates are presented in this document, with detailed outputs of representative models across all levels provided in S2 (Tables S2.1, S2.2; Figs. S2.4-S2.12). Spatial sensitivity and minimum

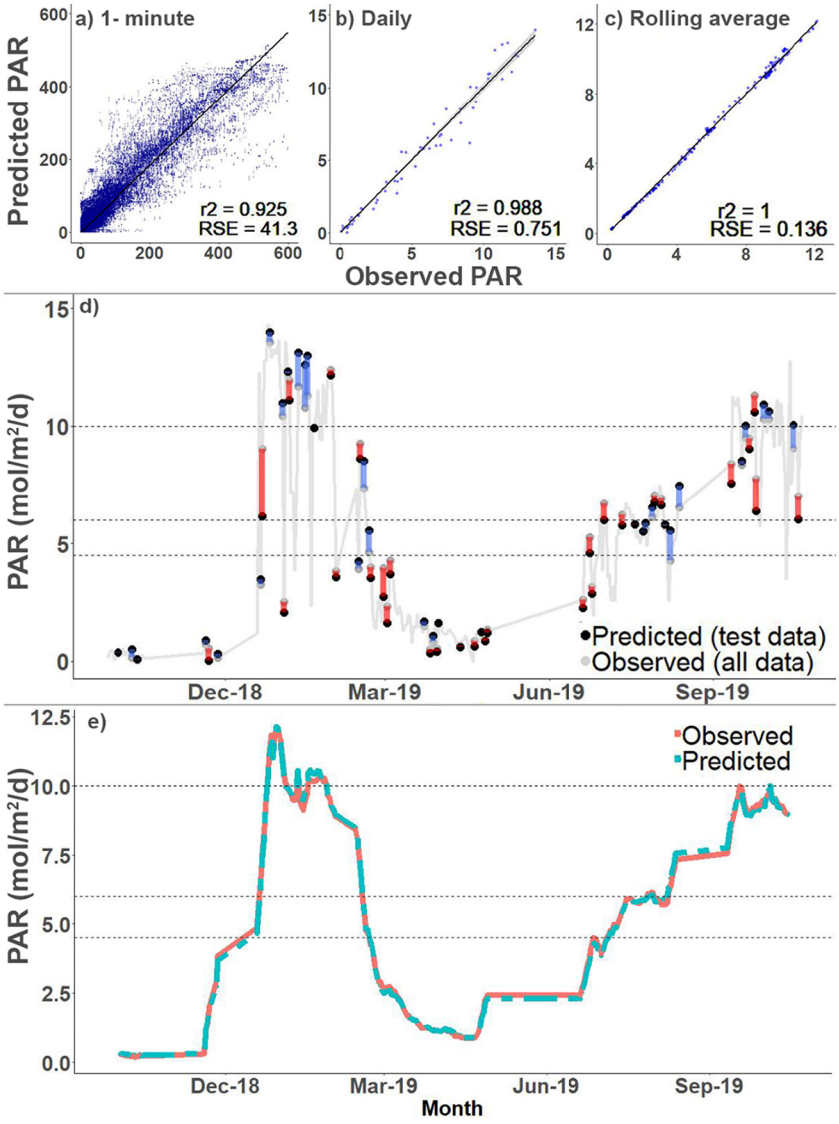

Fig. 2. Accuracy summaries for model K1 across three temporal scales. Top panel shows linear models comparing observed to predicted values at a) 1-minute scale (μmol/m^2/s); b) daily dose (mol/m^2/d); c) 14-day rolling average(mol/m^2/d); d) shows time-series plot of test data accuracy at daily level, and e) time-series plot of predicted and observed 14-day rolling average. Model K1 comparison between predicted and observed values by date at two temporal scales: a) daily, b) 14-day rolling average. In d) vertical, coloured lines represent the magnitude of differences between observed and predicted daily doses. Red lines show predictions that are lower than observation and blue show predictions that are higher. Solid pale grey line is observed values across the whole dataset. Dashed horizontal grey lines represent several light thresholds (4.5, 6, 10 mol/m^2/d) discussed in text that have been recommended for seagrass management on the Gold Coast and in other areas. (For interpretation of the references to colour in this figure legend, the reader is referred to the web version of this article.)

data requirements were assessed by plotting the error between observed and predicted for each site individually against the number of in-situ observations collected at that site.

3. Results

3.1. In-water light observations

Light intensity at the seagrass canopy varied considerably between dates and locations (Figs. 2, S2.1). Light levels through the Dec-Feb period were the highest, reaching a peak of 14.3 mol/m^2/d, whereas other periods/locations recorded near zero light intensities at times, especially at the northern extent (Figs. 2, S2.1).

3.2. Key influencers of light reaching SAV

The predictors that had the strongest effect on light availability were those related to solar intensity, time-of-year, and some physical characteristics of the location. Solar dose was the predictor that consistently returned the highest influence in the model (41.6 ± 1.1%), with distance from ocean the next most influential (32.5 ± 1.8%; Fig. 3). Depth, site aspect, and week were the only other predictors providing more than 5% influence on the model, each of these three accounting for between 6 and 9% (Fig. 3). Due to the low influence of several predictors (<2%), we also trained a set of models using only the top five ranked predictors (hereafter, 5 predictor models).

3.3. Predicting light levels from remote data

Very strong predictive accuracy was observed from almost all models. Model accuracy was always higher when assessed at coarser temporal scales (i.e. accuracy at 1 min < daily <14-day rolling average) and with a greater proportion of data used in model training. For example, the best model, designated K1, used all 11 predictors and showed a strong linear relationship between predicted and observed values at 1-minute resolution ($r^2 = 0.93$; RSE = 41.3 μmol/m^2/s or 6.9% of range in observations), which improved when data were aggregated at coarser temporal resolutions (daily $r^2 = 0.99$, RSE = 0.75 mol/m^2/d; 14-day $r^2 = 1.0$; RSE = 0.136 mol/m^2/d; Fig. 2). The K1 model returned an average 14-day rolling average accuracy of 99.3% (range 98.2 to 100.0%) when comparing whether predictions were correctly above or below each of the 11 designated thresholds. Five replications using the same model parameters (75% training data and 11 predictors), but different random separation into training/testing datasets, returned very similar results with an overall mean accuracy across 55 threshold tests (11 thresholds, 5 model replications) of 99% (range for individual thresholds within all models: 94.3 to 100%; Table S2.1).

Two-week rolling average prediction accuracy was consistently very high (>96%) for all models trained on data proportions higher than 25% (>86,011 observations; Fig. 4a). Accuracy reduced and became less consistent at training data levels between 3 and 10% (10,493–39,216 observations; Fig. 4a). In general, the 11 predictor models performed marginally, but not significantly, better than the 5 predictor models (Fig. 4), but with some exceptions at lower training data volumes. For example, at 7.5 and 10% training data volumes, the 11 predictor models appear to have been much more variable, and with lower average accuracy than the 5 predictor models. However, in both cases this was driven by inaccuracy in a single threshold level (1 mol/m^2/d), for which one model at each training volume recorded 0% accuracy.

3.4. Quantifying spatial variation in comparison to amount of monitoring data

Accuracy across separate locations was high, with mean within-site error (as difference between observed and predicted at 1-minute resolution) below 2.5% of the site-range in almost all cases (Figs. 1, S2.2). Only two locations, both with low monitoring effort returned error values higher than 5% error (red circles in Fig. 1; S2.2). One of these locations was monitored for only 49 min and, in the K1 model, returned differences between observed and predicted of 27 ± 7.6% of the observed value (mean ± SE). The other, monitored for 2098 daylight minutes, returned mean differences of 15 ± 0.8% of the observed value. However, 24 other short-term deployments (<1 week) returned very low error rates of <5%, even in deployments that were in the water for less than 2 h.

4. Discussion

We present a machine learning model that accurately predicts the light reaching SAV in the Gold Coast Broadwater, Australia. The SVLM was able to apply 'learned' information from trends identified in observation data to independent data and predict light intensity with very high accuracy, even with very low training data proportions compared to needs for other similar techniques (e.g. commonly 80%; Alexandropoulos et al., 2019). Accuracy was good at the 1-minute level, but improved with increasing temporal scale of assessment, as data were aggregated into larger time units (Fig. 2). This culminated in the best models achieving a 14-day rolling average accuracy of >99% against 11 real and potential management thresholds. Accuracy was also high across spatially separate locations (<5% mean error at 1-minute level), except at two locations (15 and 28% error, respectively) that were both monitored for very short periods (Figs. 1, S2.2). Despite these two locations returning the highest error rates, 24 other short-term deployments (<1 week) returned very high accuracies (all with errors <5%). This allows some inferences into minimum training data requirements for future applications. We found that solar dose is the major influencer in the SVLM, but that several other factors (distance from ocean; depth; site aspect; and week) also significantly influence

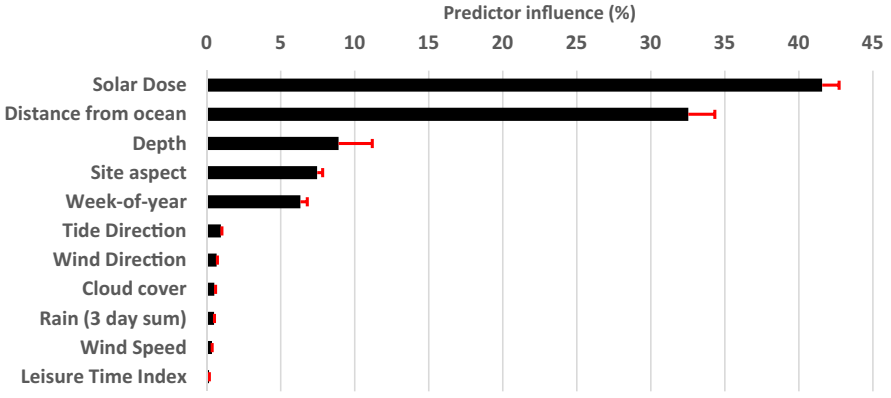

Fig. 3. The relative influence of each predictor on light observed (mean percentage + SE). Values from 5 replications of 11-predictor models with 75% of data assigned to training dataset.

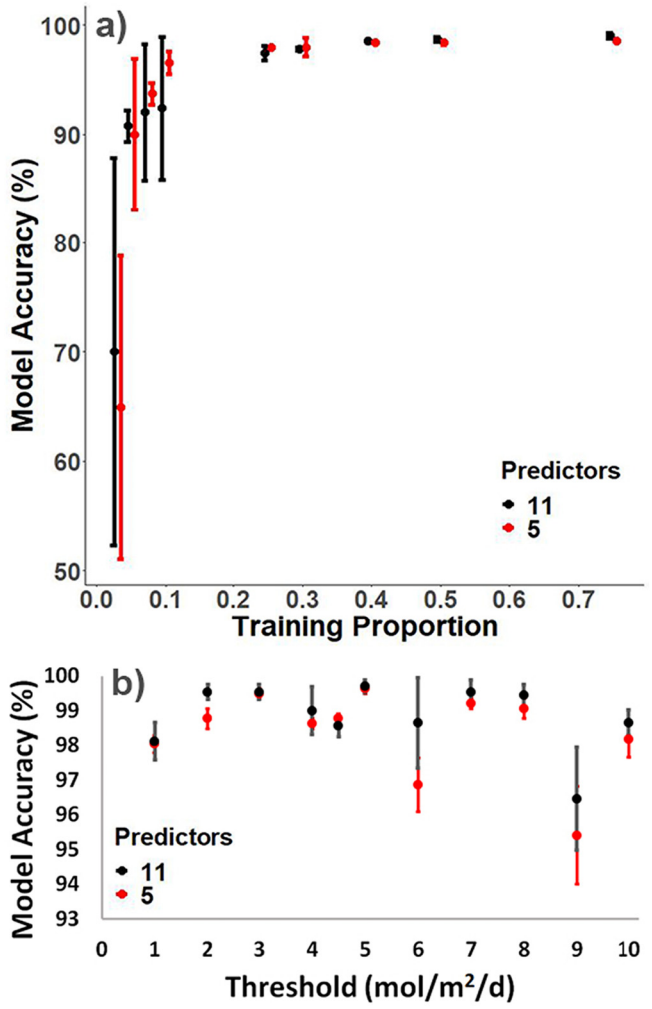

Fig. 4. Accuracy of models (mean ± SE) in correctly predicting whether the 14-day rolling average was above or below 11 hypothetical management thresholds.a) Models with varying training data volumes. X-axis represents the proportion of days in the full dataset that were assigned to training the model.. b): Accuracy at each threshold for models trained on 75% of data with 11 (black; $N = 5$) and 5 predictors (red; $N = 3$). Models using only five predictors were processed using only the predictors with the the highest influence (mean > 5%) in the 11-predictor models: solar dose; distance to ocean; week; depth; and site aspect. (For interpretation of the references to colour in this figure legend, the reader is referred to the web version of this article.)

light reaching SAV. While very important for estimating PAR, changes in solar dose alone are unlikely to be the major cause of light-stress to submerged vegetation, with many other potential factors more likely to force light below needs (e.g. Dixon, 1999). Thus, despite comparatively lower influence on observed light intensities, the other predictors in the SVLM provide valuable insight into the likely causes of light-stress in the region.

Our analyses of data volume used to train the models suggests that minimal, but strategic, in-water monitoring could be sufficient to train a similarly accurate model in new areas if available predictor data are sufficient to explain light. For example, the model returned better than 90% accuracy in 5/6 replications when trained with only 7.5% of days (24 days total) from the full 241-day dataset, and better than 96% when trained on data volumes ≥25% (Fig. 4). We believe this high accuracy was only achievable because the in-water observations spanned approximately 1-year, accounting for the full range of weeks in the year, and because conditions in the other predictor data varied considerably throughout this time, thus providing a sufficient variety of training conditions. In cases where training data fails to encompass the range of potential values in predictor data, the model can have trouble extrapolating (Hooker, 2004). For example, the 1-year model training data included a severe storm, suggesting that the SVLM should therefore be sensitive to future storm events. Thus, we suggest that periodically collected in-water data that span approximately one full year may be sufficient to train an accurate SVLM containing a time-of-year predictor (i.e. week). While untested thus far, under these conditions, and in the absence of large-scale changes to dynamics within the system we may expect that predictions in future years will be similarly accurate. But this would require some ongoing validation effort. It is feasible that future changes to system dynamics (e.g. nearby land-use and climactic cycles) may trigger changes to how some predictors (e.g. rainfall, wind speed and direction) interact to affect how predictors impact light penetration. This suggests that periodic model maintenance could benefit longer-term predictive accuracy. For example, future monitoring data collected at different times of year, or following major changes to system dynamics, could be used to re-train the SVLM. Incorporating future changes in predictor dynamics into the model in this way may provide ongoing confidence in the precision with which the SVLM can predict light intensity.

While we do not suggest that the SLVM, trained on Gold Coast data, is directly transferrable to other areas, the general approach in selecting predictor variables and training a machine-learning model could be used successfully in other locations. The most suitable predictors and the relative influence of each predictor will likely vary in new areas based on locally important factors. Places with strong pulsed influences from river input or a range of specific point source inputs, for example, may need to have these variables included for accurate model development. Conversely, some of the local factors that are important for the Gold Coast setting may not be as influential elsewhere. For example, the distance-to-ocean predictor is unlikely to be useful in unsheltered locations that are directly exposed to oceanic waters or situated much farther inland, with little or no tidal influence. The success of our model was also highly reliant on the availability of solar exposure data for the location. The availability of similar measurements of incident light for other locations will be critical in the successful application of the modelling approach elsewhere.

4.1. Potential applications

Light stress represents a major threat to SAV globally (Orth et al., 2006; O'Brien et al., 2018; Wu et al., 2018), so an ability to remotely quantify PAR at the SAV canopy and identify the cause of excursions below light thresholds can benefit the management and conservation of these important ecosystems. Environmental pressure information is essential in holistic ecosystem-based assessment and management (Borja et al., 2008; Roca et al., 2016). Changes in light intensity can be used for understanding changes in the condition and trend of SAV, and so the SVLM could be applied in routine monitoring and assessment. Near real-time remote estimation of light intensity can be used to assess excursions below thresholds and can also identify SAV at risk of light stress (sensu Collier et al., 2012a, Choice et al., 2014, Collier et al., 2016a, Chartrand et al., 2018). The SVLM, can be applied as a spatial tool, identifying habitat suitability and at-risk areas. This can provide environmental managers with an early warning of potential declines in SAV growth and survival, and to stratify monitoring design, focussing on areas with high levels of risk.

The SVLM may also allow forecasting of benthic PAR, alongside the hindcasting capabilities we have demonstrated here. The consistency in prediction accuracy shown by these models, alongside the ability to forecast trends in many predictors (e.g. rainfall, wind, solar radiation), means it is possible to now hindcast, but feasibly also forecast benthic PAR/light conditions by estimating future values for each predictor and applying them to the SVLM. This represents a potential future research avenue with strong management implications.

The SVLM contributes to empowering managers to employ an adaptive management plan that both minimises activity downtime and also

protects SAV (Ventín et al., 2015; Maxwell et al., 2017). As an example, the SVLM could be used in the implementation of dredge management plans, or to mitigate other acute disturbances to the light environment. We use dredging as an example because this activity is known to acutely impact light penetration in a way that affects the health of SAV and is routinely monitored and reported upon. We suggest that the SVLM can be used to assess the effect of dredging and other human activities and inform mitigation strategies both before and during operation. Reference conditions provide a baseline or target against which to assess the effects of activities, such as dredging, on light intensity. Reference conditions can be based on historical (pre-activity) conditions, or reference sites, for example, each with their benefits and drawbacks (Borja et al., 2012). The 14-day rolling average, for which the SVLM obtained the best predictive accuracy, is often used to trigger sand-management mitigation actions, making this resolution potentially the most management-relevant level to compare with reference conditions. In the hypothetical scenario illustrated in Fig. 5, predictions accurately match in-water observations before the activity begins, thus confirming prediction accuracy and assessing pre-activity conditions against management thresholds. Once the activity starts, the in-water observation values then drop below the management threshold, whereas the SVLM predictions remain above. This would suggest that the activity is having a negative effect on light penetration to the point of causing light-stress. Managers monitoring this area could respond to differences between in-situ measurements and SVLM estimates during a dredging activity, potentially triggering mitigation actions that improve light levels to minimise SAV loss (e.g. Chartrand et al., 2016). Similarly, where the SVLM predicts that light is below management thresholds independent of the dredging activity, managers could infer that the activity is unlikely to be having any additional impact on SAV. This type of management support tool would allow for reference conditions to be estimated directly at the affected location, rather than at an alternative reference location that may unexpectedly respond differently to changed conditions. Thus, the SVLM can directly support management and conservation efforts while minimising cost and risk to personnel.

Furthermore, where multiple sites near SAV are to be dredged, the dredge provider or management authority could use the SVLM to model light conditions at all sites simultaneously, avoiding areas where the activity is likely to lengthen light-stress, and instead focusing effort in areas where dredging induced light reductions are unlikely to breach thresholds. While it is likely that some level of in-situ measurement of PAR would still be required for legislative compliance purposes, and for validating the accuracy of the SVLM during works, the ability to extend the spatial range of benthic PAR assessments via the SVLM would allow a much more robust management approach without the requirement to have in-situ loggers located everywhere impacts may occur. If it were also possible to forecast (at daily or longer time resolutions) that natural light would be above or below a particular management threshold in one place, then management activities could be planned around timeframes expected to have minimal impact.

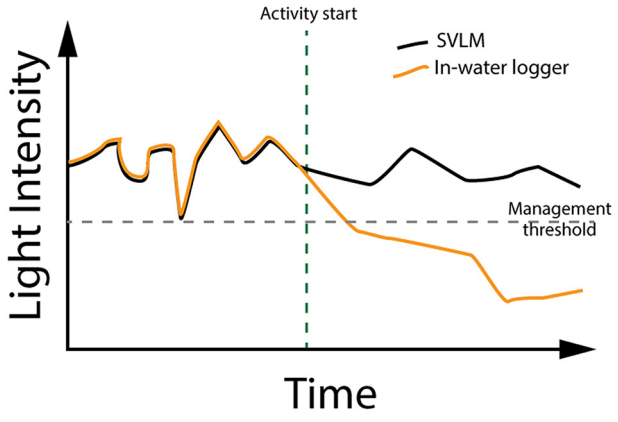

Fig. 5. Hypothetical use of SVLM to quantify the effect of human activities. This example compares light measured in-situ before the activity begins with the SVLM predictions to both assess whether measure pre-activity conditions have provided suitable light and confirm accuracy of SVLM. Then, an estimate of the effect of the activity can be calculated by comparing expected 'natural' (SVLM) light values to those affected by the activity in the exact same location (rather than an alternative reference location that may not be exposed to identical conditions).

5. Conclusions

We use remotely available data to assess the influence of different drivers on light levels (PAR), and to create a predictive model (the SVLM) that allows remote estimation of the light environment from remotely available data. We were able to assess the influence of various environmental and anthropogenic drivers on light reaching submerged vegetation and develop a robust predictive model that accurately estimates light levels with >99% accuracy at our study location. This powerful technique could feasibly be applied anywhere that suitable remote predictor data are available, providing the capacity to disentangle the influence of different pressures on light availability, and to hindcast or forecast light conditions in future assessments and management applications. Application of the SVLM technique could also minimise reliance on in-water instruments (beyond collection of training data and validation of models in new regions and sentinel sites during management of activities), and provide time-series data and better spatial coverage of benthic PAR for management applications.

CRediT authorship contribution statement

Ryan M. Pearson: Conceptualization, Methodology, Validation, Formal analysis, Investigation, Data curation, Writing – original draft, Writing – review & editing, Visualization, Supervision, Project administration, Funding acquisition. **Catherine J. Collier:** Conceptualization, Writing – review & editing, Visualization, Funding acquisition. **Christopher J. Brown:** Methodology, Formal analysis, Writing – review & editing, Visualization. **Michael A. Rasheed:** Conceptualization, Writing – review & editing, Visualization, Funding acquisition. **Jessica Bourner:** Writing – review & editing, Project administration, Funding acquisition. **Mischa P. Turschwell:** Formal analysis, Writing – review & editing, Visualization. **Michael Sievers:** Writing – review & editing, Visualization. **Rod M. Connolly:** Conceptualization, Methodology, Writing – review & editing, Visualization, Supervision, Project administration, Funding acquisition.

Declaration of competing interest

The authors declare that they have no known competing financial interests or personal relationships that could have appeared to influence the work reported in this paper.

Acknowledgements

This project was funded by the Gold Coast Waterways Authority, Australia (GCWA 22000-008) and the Global Wetlands Project, supported by a charitable organization which neither seeks nor permits publicity for its efforts. The authors thank the following people for assistance with fieldwork, access to equipment, data processing and analyses: E. Ditria, M. Campbell, H. van Woerden, C. Bryant, Z. Parkes, Z. Carey, J. Gustafson, J. Krueger, L. Hughes, A. Giffin, F. Connolly, and T. Rayner.

Appendix A. Supplementary data

Supplementary data to this article can be found online at https://doi.org/10.1016/j.scitotenv.2021.146886.

References

Adams, M.P., Hovey, R.K., Hipsey, M.R., Bruce, L.C., Ghisalberti, M., Lowe, R.J., Gruber, R.K., Ruiz-Montoya, L., Maxwell, P.S., Callaghan, D.P., 2016. Feedback between sediment and light for seagrass: where is it important? Limnol. Oceanogr. 61, 1937–1955.

Alexandropoulos, S.-A.N., Aridas, C.K., Kotsiantis, S.B., Vrahatis, M.N., 2019. Multi-objective evolutionary optimization algorithms for machine learning: a recent survey. Approximation and Optimization. Springer.

Álvarez-Romero, J.G., Devlin, M., da Silva, E.T., Petus, C., Ban, N.C., Pressey, R.L., Kool, J., Roberts, J.J., Cerdeira-Estrada, S., Wenger, A.S., 2013. A novel approach to model exposure of coastal-marine ecosystems to riverine flood plumes based on remote sensing techniques. J. Environ. Manag. 119, 194–207.

Anthony, K.R., Ridd, P.V., Orpin, A.R., Larcombe, P., Lough, J., 2004. Temporal variation of light availability in coastal benthic habitats: effects of clouds, turbidity, and tides. Limnol. Oceanogr. 49, 2201–2211.

Baird, M.E., Adams, M.P., Babcock, R.C., Oubelkheir, K., Mongin, M., Wild-Allen, K.A., Skerratt, J., Robson, B.J., Petrou, K., Ralph, P.J., O'Brien, K.R., Carter, A.B., Jarvis, J.C., Rasheed, M.A., 2016. A biophysical representation of seagrass growth for application in a complex shallow-water biogeochemical model. Ecol. Model. 325, 13–27.

Borja, A., Bricker, S.B., Dauer, D.M., Demetriades, N.T., Ferreira, J.G., Forbes, A.T., Hutchings, P., Jia, X., Kenchington, R., Marques, J.C., 2008. Overview of integrative tools and methods in assessing ecological integrity in estuarine and coastal systems worldwide. Mar. Pollut. Bull. 56, 1519–1537.

Borja, Á., Dauer, D.M., Grémare, A., 2012. The importance of setting targets and reference conditions in assessing marine ecosystem quality. Ecol. Indic. 12, 1–7.

Brown, C.J., Broadley, A., Adame, M.F., Branch, T.A., Turschwell, M.P., Connolly, R.M., 2019. The assessment of fishery status depends on fish habitats. Fish Fish. 20, 1–14.

Chartrand, K.M., Bryant, C.V., Carter, A.B., Ralph, P.J., Rasheed, M.A., 2016. Light thresholds to prevent dredging impacts on the Great Barrier Reef seagrass, Zostera muelleri ssp. capricorni. Front. Mar. Sci. 3, 106.

Chartrand, K.M., Szabó, M., Sinutok, S., Rasheed, M.A., Ralph, P.J., 2018. Living at the margins – the response of deep-water seagrasses to light and temperature renders them susceptible to acute impacts. Mar. Environ. Res. 136, 126–138.

Choice, Z.D., Frazer, T.K., Jacoby, C.A., 2014. Light requirements of seagrasses determined from historical records of light attenuation along the Gulf coast of peninsular Florida. Mar. Pollut. Bull. 81, 94–102.

City of Gold Coast, 2019. Gold Coast Estimated Resident Population (ERP) as at 30/6/2019 (Gold Coast, Australia).

Coffer, M.M., Schaeffer, B.A., Zimmerman, R.C., Hill, V., Li, J., Islam, K.A., Whitman, P.J., 2020. Performance across WorldView-2 and RapidEye for reproducible seagrass mapping. Remote Sens. Environ. 250, 112036.

Collier, C., Waycott, M., McKenzie, L., 2012a. Light thresholds derived from seagrass loss in the coastal zone of the northern Great Barrier Reef, Australia. Ecol. Indic. 23, 211–219.

Collier, C., Chartrand, K., Honchin, C., Fletcher, A., Rasheed, M., 2016a. Light Thresholds for Seagrasses of the GBRWHA: a Synthesis and Guiding Document. 41. Report to the National Environmental Science Programme Reef and Rainforest Research Centre Limited, Cairns, QLD, Australia.

Collier, C.J., Waycott, M., Ospina, A.G., 2012b. Responses of four indo-West Pacific seagrass species to shading. Mar. Pollut. Bull. 65, 342–354.

Collier, C.J., Adams, M.P., Langlois, L., Waycott, M., O'Brien, K.R., Maxwell, P.S., McKenzie, L., 2016b. Thresholds for morphological response to light reduction for four tropical seagrass species. Ecol. Indic. 67, 358–366.

Connolly, R.M., Dunn, R.J.K., Kovacs, E.M., Maxwell, P.S., McKenna, S.A., Phinn, S.R., Rasheed, M.A., Roelfsema, C.M., York, P.H., 2016. Marine Plant Habitat and Monitoring Program (SRMP-002). Report to Gold Coast Waterways Authority. Griffith University, Gold Coast, Australia.

Cuttriss, A.K., Prince, J.B., Castley, J.G., 2013. Seagrass communities in southern Moreton Bay, Australia: coverage and fragmentation trends between 1987 and 2005. Aquat. Bot. 108, 41–47.

Dixon, L.K., 1999. Establishing light requirements for the seagrass *Thalassia testudinum*: an example from Tampa Bay, Florida. Seagrasses. CRC Press.

Elith, J., Leathwick, J., 2017. Boosted Regression Trees for ecological modeling. R documentation Available at. https://cran.r-project.org/web/packages/dismo/vignettes/brt.pdf.

Erftemeijer, P.L., Shuail, D.A., 2012. Seagrass habitats in the Arabian Gulf: distribution, tolerance thresholds and threats. Aquat. Ecosyst. Health Manag. 15, 73–83.

Fernandes, M.B., Daly, R., van Gils, J., Kildea, T., Caires, S., Erftemeijer, P.L.A., 2018. Parameterization of an optical model to refine seagrass habitat requirements in an urbanized coastline. Estuar. Coast. Shelf Sci. 207, 471–482.

Fernandes, M.B., van Gils, J., Erftemeijer, P.L., Daly, R., Gonzalez, D., Rouse, K., 2019. A novel approach to determining dynamic nitrogen thresholds for seagrass conservation. J. Appl. Ecol. 56, 253–261.

Ganju, N.K., Miselis, J.L., Aretxabaleta, A.L., 2014. Physical and biogeochemical controls on light attenuation in a eutrophic, back-barrier estuary. Biogeosciences 11, 7193–7205. https://doi.org/10.5194/bg-11-7193-2014.

Garrad, P., Hey, R., 1987. Boat traffic, sediment resuspension and turbidity in a Broadland river. J. Hydrol. 95, 289–297.

Greenwell, B., Boehmke, B., Cunningham, J., GBM Developers, 2019. gbm: generalized boosted regression models. R Package Version 2.1.5 https://CRAN.R-project.org/package=gbm.

Hooker, G., 2004. Diagnostics and Extrapolation in Machine Learning. Stanford University.

Kerimoglu, O., Große, F., Kreus, M., Lenhart, H.J., van Beusekom, J.E.E., 2018. A model-based projection of historical state of a coastal ecosystem: relevance of phytoplankton stoichiometry. Sci. Total Environ. 639, 1311–1323.

Kilminster, K., McMahon, K., Waycott, M., Kendrick, G.A., Scanes, P., McKenzie, L., O'Brien, K.R., Lyons, M., Ferguson, A., Maxwell, P., Glasby, T., Udy, J., 2015. Unravelling complexity in seagrass systems for management: Australia as a microcosm. Sci. Total Environ. 534, 97–109.

Lawson, S., Wiberg, P., McGlathery, K., Fugate, D., 2007. Wind-driven sediment suspension controls light availability in a shallow coastal lagoon. Estuar. Coasts 30, 102–112.

Lee, K.-S., Park, S.R., Kim, Y.K., 2007. Effects of irradiance, temperature, and nutrients on growth dynamics of seagrasses: a review. J. Exp. Mar. Biol. Ecol. 350, 144–175.

Leon, L.M., Warnken, J., 2008. Copper and sewage inputs from recreational vessels at popular anchor sites in a semi-enclosed bay (Qld, Australia): estimates of potential annual loads. Mar. Pollut. Bull. 57, 838–845.

de los Santos, C.B., Krause-Jensen, D., Alcoverro, T., Marbà, N., Duarte, C.M., van Katwijk, M.M., Pérez, M., Romero, J., Sánchez-Lizaso, J.L., Roca, G., Jankowska, E., Pérez-Lloréns, J.L., Fournier, J., Montefalcone, M., Pergent, G., Ruiz, J.M., Cabaço, S., Cook, K., Wilkes, R.J., Moy, F.E., Trayter, G.M.-R., Arañó, X.S., de Jong, D.J., Fernández-Torquemada, Y., Auby, I., Vergara, J.J., Santos, R., 2019. Recent trend reversal for declining European seagrass meadows. Nat. Commun. 10, 3356.

Magno-Canto, M.M., McKinna, L.I., Robson, B.J., Fabricius, K.E., 2019. Model for deriving benthic irradiance in the Great Barrier Reef from MODIS satellite imagery. Opt. Express 27, A1350–A1371.

Maxwell, P.S., Pitt, K.A., Burfeind, D.D., Olds, A.D., Babcock, R.C., Connolly, R.M., 2014. Phenotypic plasticity promotes persistence following severe events: physiological and morphological responses of seagrass to flooding. J. Ecol. 102, 54–64.

Maxwell, P.S., Eklöf, J.S., van Katwijk, M.M., O'Brien, K.R., de la Torre-Castro, M., Boström, C., Bouma, T.J., Krause-Jensen, D., Unsworth, R.K.F., van Tussenbroek, B.I., van der Heide, T., 2017. The fundamental role of ecological feedback mechanisms for the adaptive management of seagrass ecosystems – a review. Biol. Rev. 92, 1521–1538.

McMahon, K., Collier, C., Lavery, P.S., 2013. Identifying robust bioindicators of light stress in seagrasses: a meta-analysis. Ecol. Indic. 30, 7–15.

O'Brien, K.R., Adams, M.P., Ferguson, A.J., Samper-Villarreal, J., Maxwell, P.S., Baird, M.E., Collier, C., 2018. Seagrass Resistance to Light Deprivation: Implications for Resilience. Springer, Seagrasses of Australia.

Orth, R.J., Carruthers, T.J.B., Dennison, W.C., Duarte, C.M., Fourqurean, J.W., Heck, K.L., Hughes, A.R., Kendrick, G.A., Kenworthy, W.J., Olyarnik, S., Short, F.T., Waycott, M., Williams, S.L., 2006. A global crisis for seagrass ecosystems. BioScience 56, 987–996.

Pearson, R.M., Collier, C.J., Rasheed, M.A., Bryant, C.V., Connolly, R.M., 2020. Light Threshold Requirements for Seagrasses in the Gold Coast Waterways. Report to Gold Coast Waterways Authority. Griffith University, Gold Coast, Australia.

Roca, G., Alcoverro, T., Krause-Jensen, D., Balsby, T.J.S., van Katwijk, M.M., Marba, N., Santos, R., Arthur, R., Mascaro, O., Fernandez-Torquemada, Y., Perez, M., Duarte, C.M., Romero, J., 2016. Response of seagrass indicators to shifts in environmental stressors: a global review and management synthesis. Ecol. Indic. 63, 310–323.

Roelfsema, C.M., Lyons, M., Kovacs, E.M., Maxwell, P., Saunders, M.I., Samper-Villarreal, J., Phinn, S.R., 2014. Multi-temporal mapping of seagrass cover, species and biomass: a semi-automated object based image analysis approach. Remote Sens. Environ. 150, 172–187.

Scott, A.L., York, P.H., Duncan, C., Macreadie, P.I., Connolly, R.M., Ellis, M.T., Jarvis, J.C., Jinks, K.I., Marsh, H., Rasheed, M.A., 2018. The role of herbivory in structuring tropical seagrass ecosystem service delivery. Front. Plant Sci. 9, 127.

Sievers, M., Brown, C.J., Tulloch, V.J.D., Pearson, R.M., Haig, J.A., Turschwell, M.P., Connolly, R.M., 2019. The role of vegetated coastal wetlands for marine megafauna conservation. Trends Ecol. Evol. 34 (9), 807–817. https://doi.org/10.1016/j.tree.2019.04.004.

Sievers, M., Pearson, R.M., Turschwell, M.P., Bishop, M.J., Bland, L., Brown, C.J., Tulloch, V.J.D., Haig, J.A., Olds, A.D., Maxwell, P.S., Connolly, R.M., 2020. Integrating outcomes of IUCN red list of ecosystems assessments for connected coastal wetlands. Ecol. Indic. 116, 106489.

Ventín, L.B., de Souza, Troncoso J., Villasante, S., 2015. Towards adaptive management of the natural capital: disentangling trade-offs among marine activities and seagrass meadows. Mar. Pollut. Bull. 101, 29–38.

Waycott, M., Duarte, C.M., Carruthers, T.J., Orth, R.J., Dennison, W.C., Olyarnik, S., Calladine, A., Fourqurean, J.W., Heck, K.L., Hughes, A.R., 2009. Accelerating loss of seagrasses across the globe threatens coastal ecosystems. Proc. Natl. Acad. Sci. 106, 12377–12381.

Wu, P.P.Y., McMahon, K., Rasheed, M.A., Kendrick, G.A., York, P.H., Chartrand, K., Caley, M.J., Mengersen, K., 2018. Managing seagrass resilience under cumulative dredging affecting light: predicting risk using dynamic Bayesian networks. J. Appl. Ecol. 55, 1339–1350.

Yaakub, S.M., Chen, E., Bouma, T.J., Erftemeijer, P.L., Todd, P.A., 2014. Chronic light reduction reduces overall resilience to additional shading stress in the seagrass Halophila ovalis. Mar. Pollut. Bull. 83, 467–474.

York, P.H., Carter, A.B., Chartrand, K., Sankey, T., Wells, L., Rasheed, M.A., 2015. Dynamics of a deep-water seagrass population on the great barrier reef: annual occurrence and response to a major dredging program. Sci. Rep. 5, 13167.

Zoffoli, M.L., Gernez, P., Rosa, P., Le Bris, A., Brando, V.E., Barillé, A.-L., Harin, N., Peters, S., Poser, K., Spaias, L., Peralta, G., Barillé, L., 2020. Sentinel-2 remote sensing of Zostera noltei-dominated intertidal seagrass meadows. Remote Sens. Environ. 251, 112020.